Nucleic Acids Research, 2025, **53**, gkae1280
https://doi.org/10.1093/nar/gkae1280
Advance access publication date: 8 January 2025
Chemical Biology and Nucleic Acid Chemistry

One-pot ligation of multiple mRNA fragments on dsDNA splint advancing regional modification and translation

Yunfan Xu [1,†], Shuopeng Qi [1,†], Gongrui Zhang [1], Dan Liu [1], Dejin Xu [1], Tong Qin [1], Qin Cheng [1], Han Kang [1], Bei Hu [1,*] and Zhen Huang [1,2,*]

[1]Key Laboratory of Bio-resource and Eco-environment of Ministry of Education, The College of Life Sciences, Sichuan University, 24 South Section 1, 1st Ring Road, Chengdu, Sichuan 610064, P.R. China
[2]SeNA Research Institute, School of Life Sciences, Hubei University, 368 Youyi Avenue, Wuhan, Hubei 430062, P.R. China

[*]To whom correspondence should be addressed. Tel: +86 28 85502629; Fax: +001 404 4135535; Email: huang@senaresearch.org
Correspondence may also be addressed to Bei Hu. Tel: +86 28 85502629; Email: hubei@scu.edu.cn
[†]The first two authors should be regarded as Joint First Authors.

Abstract

Region-specific RNA modifications are crucial for advancing RNA research and therapeutics, including messenger RNA (mRNA)-based vaccines and immunotherapy. However, the predominant method, synthesizing regionally modified mRNAs with short single-stranded DNA (ssDNA) splints, encounters challenges in ligating long mRNA fragments due to the formation of RNA self-folded complex structures. To address this issue, we developed an efficient strategy using an easily obtained long double-stranded DNA (dsDNA) as a ligation splint after *in situ* denaturing, while parts of this dsDNA are the templates for transcribing mRNA fragments. We observed that the denatured dsDNA formed a long hybrid duplex with these mRNA fragments, overcoming their structures. Further, our novel strategy remarkably facilitated the ligation of long mRNA fragments (especially structured ones), offering ligation efficiency up to 106-fold higher than the ssDNA method. Using this one-pot strategy, we conveniently synthesized the mRNAs with N^1-methylpseudouridine ($m^1\psi$) and 5-methylcytidine (m^5C) modifications in specific regions. We have found that compared with the fully modified mRNAs, the 3′UTR $m^1\psi$ modifications alone increased the translation efficiency, and the combined modifications of the $m^1\psi$-3′UTR and m^5C-5′UTR/CDS exhibited higher translation efficiency and lower immunogenicity in general. Our study presents a broadly applicable strategy for producing regionally modified mRNAs, advancing the potential of mRNA therapeutics.

Graphical abstract

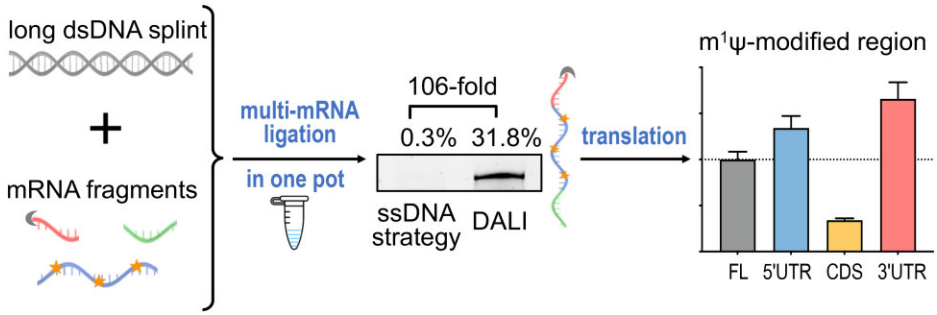

Introduction

Messenger RNA (mRNA) therapy (an emerging category of therapeutics) is revolutionizing disease treatment paradigms (1), encompassing infectious disease vaccines (2,3), cancer immunotherapies (4,5), protein replacement therapies (6) and genetic disease treatment (7). Unfortunately, unmodified mRNA is inherently unstable and immunogenic (1,8,9). To address these challenges, many modifications have been developed, such as N^1-methylpseudouridine ($m^1\psi$), 5-methyluridine, 5-methoxyuridine, 5-methylcytidine (m^5C) and 6-methyladenine (1,10,11). Among these, $m^1\psi$ has been proven effective in mRNA therapeutics, which were first successfully used as vaccines against the COVID-19 epidemic, saving tens of millions of lives (12,13). The modified mRNA therapeutics are traditionally prepared by *in vitro* transcription (IVT) by using modified nucleoside triphosphates (NTPs), resulting in global modifications (8,14). However, it was recently reported that these mRNA vaccines modified with $m^1\psi$ globally could result in unavoidable drawbacks, such as +1 ribosomal frameshifting in the coding sequence (CDS) and reduced translation speed (15). Likewise, globally derivatized mRNAs with other modifications could cause similar issues,

Received: April 17, 2024. **Revised:** December 9, 2024. **Editorial Decision:** December 11, 2024. **Accepted:** December 18, 2024

reducing translation efficiency and posing potential health risks. Therefore, region-specific modifications in mRNAs are essential for developing high-quality therapeutics.

To achieve the regional modification of mRNA, ligation-based strategies have been developed either chemically or enzymatically (16). Chemical ligations of long RNA are often involved in nonspecific activation and ligation, poor ligation efficiency or unnatural bond formation (17,18), compromising mRNA functions and applications. In contrast, the enzymatic method is better for long RNA synthesis via structure-free-end ligation or nicked-end ligation assisted by a splint (external or self-splinted one) (19–21). Compared with structure-free-end ligation, nick RNA ligation on a splint is preferred due to the high specificity (20,22). Obviously, external-splint ligation has unlimited choices on ligation sites, while self-splinted ligation has limited choices (23,24).

The canonical approach typically utilizes a short synthetic single-stranded oligonucleotide DNA (<100 nt) as a splint (22,25), which works efficiently for ligating short and unstructured RNAs, but not for ligating multiple or long mRNA fragments (26). We hypothesized that the low ligation efficiency is likely due to the folding and structures of long mRNA fragments. Thus, we have proposed a solution to address the problem by using a long splint to compete with these structures. However, synthesizing long single-stranded DNA (ssDNA) splints (>1000 nt) is challenging via chemical methods (27), and is labor-intensive via biological methods (28,29). We reasoned that a long ssDNA splint can be generated via thermo-denaturing long double-stranded DNA (dsDNA) and form a more stable RNA/DNA duplex (30,31) via annealing. Therefore, to avoid the challenges of the long splint synthesis, we have developed a strategy to easily *in situ* generate ssDNAs by denaturing dsDNAs (referred to as the dsDNA splint), providing the splints to form long RNA/DNA duplexes with mRNA fragments.

In this work, we reported the novel strategy termed long-dsDNA-splinted multi-mRNA-fragment ligation (DALI), which is highly efficient in synthesizing regionally and specifically modified mRNAs. Using this approach, we conveniently synthesized many regionally modified mRNAs with up to a 106-fold increase in ligation efficiency. By studying these mRNAs, we discovered that compared to the globally and canonically $m^1\psi$-modified mRNA, the mRNA modified on the 3′UTR region translated proteins with higher efficiency (increased by 66%; with possibly higher accuracy), while those $m^1\psi$-modified on the coding region translated with lower efficiency. Further, the observed immunogenicity caused by the unmodified region inspired us to explore a mixed modification strategy using $m^1\psi$ and m^5C in proper mRNA regions. Excitingly, the mRNAs with $m^1\psi$-modified 3′UTR and m^5C-modified 5′UTR/CDS achieved both higher translation efficiency and lower immunogenicity, presenting a potential modification pattern. Therefore, based on our experimental investigations, we have concluded that regional and specific modifications of mRNAs are critical for mRNA functions and therapeutic discoveries.

Materials and methods

Cells and reagent

Human cervical squamous cell carcinoma cells (SiHa) were obtained from the China Cell Bank and cultured in Dulbecco's Modified Eagle's Medium (DMEM; Gibco) supplemented with 10% fetal bovine serum (Yeasen), 100 units/ml penicillin (Biosharp) and 100 μg/ml streptomycin (Biosharp). The cells were maintained in a 37°C humidified incubator with a 5% CO_2 atmosphere. Solvents and reagents, primarily sourced from Sigma–Aldrich and J&K Scientific, were used as received without additional purification.

Plasmid construction

Gene sequences, comprising noncoding regions (T7 promoter, EMCV-IRES, 5′UTRs and 3′UTRs) and coding regions (including Gaussia luciferase and LuxSit-i luciferase), were synthesized by Tsingke Biotech. These sequences were then integrated into the corresponding backbone plasmid (pUC57) using a cloning kit (Uniclone One Step Seamless Cloning Kit, Genesand), constructing the plasmids for generating transcription templates and ligation splints (sequences detailed in Supplementary Tables S1 and S2, respectively).

Synthesis of transcription templates and ligation splints

Transcription templates and ligation splints were synthesized via polymerase chain reaction (PCR) using 0.01 ng/μl of DNA plasmid, 1× PrimeSTAR Max Premix (Takara Bio) and 0.8 μM primers (sequences listed in Supplementary Table S3). The thermocycling conditions were amplification for 30 cycles, including denaturing at 98°C for 10 s, annealing at 50–60°C for 10 s and extension at 72°C for 0.5–3 min based on the amplicon length. The resulting products were subjected to analysis and purification through agarose electrophoresis and the Cycle Pure Kit (Omega), respectively. In addition, chemically synthesized ssDNA splints were produced by Tsingke Biotech (sequences detailed in Supplementary Table S2).

RNA synthesis via *in vitro* transcription

T7 RNA polymerase was expressed and purified following the established protocols (32). IVT reactions were conducted with DNA templates, 5 mM each of ATP, CTP (or m^5CTP), GTP and UTP (or $m^1\psi TP$), the IVT buffer [40 mM 4-(2-hydroxyethyl)piperazine-1-ethanesulfonic acid (HEPES; pH 8.5), 40 mM dithiothreitol (DTT), 10 mM NaOAc, 75 mM $Mg(OAc)_2$ and 0.2 mM spermidine] and T7 RNA polymerase (0.1 mg/ml) at 37°C for 2 h. For synthesizing 5′-monophosphorylated RNA, GMP (4 mM) was supplemented, and the canonical GTP was reduced to 0.8 mM (21,22). For synthesizing 5′-capped RNA, the cap analog (CleanCap Reagent AG from TriLink; 4 mM) was supplemented in the transcriptional reaction mixture. Crude transcripts underwent DNase I treatment (2 U per 1 μg DNA; NEB) at 37°C for 15 min to digest DNA templates, followed by RNA precipitation with lithium chloride (LiCl, 2.5 M).

mRNA/dsDNA hybridization experiments

Unless in optimization tests, the experiments were performed as follows. The mRNA substrates (1 pM each) and the corresponding splint dsDNA (1 pM) were mixed in an annealing buffer (Beyotime). The hybridization reaction was performed by denaturing at 90°C for 1 s, followed by slow annealing to 25°C at a rate of 0.02°C/s. The hybrid formation was confirmed by RNA digestion with RNase H (NEB) or DNA digestion with DNase I (NEB), respectively. All samples were

analyzed via nondenaturing polyacrylamide gel electrophoresis (PAGE). Then, the gels were stained with Ultra GelRed (Vazyme).

RNA ligation

Following the hybridization as described above, the ligation reactions were performed with the annealed mixture, T4 RNA ligase 2 (T4 Rnl2, 0.4 U/μl; Beyotime) and the ligation buffer (50 mM Tris–HCl, pH 7.5; 2 mM $MgCl_2$; 1 mM DTT; and 0.4 mM ATP) at 25°C for 2 h. Subsequently, DNase I (2 U per 1 μg DNA; NEB) treatment was employed to digest the splint DNA with two 30-min incubations at 37 and 55°C, successively.

PAGE analysis of RNA

Nondenaturing PAGE gels [5% polyacrylamide, 1× TBE buffer, 0.1% APS, 0.01% N,N,N′,N′-tetramethylethylenediamine (TEMED)] or urea-PAGE gels (supplementing 8 M urea into nondenaturing PAGE gels) were used for RNA separation. Samples were mixed with 2× RNA loading solution or 2× RNA urea loading solution and subjected to nondenaturing (on ice) or urea-denaturing (at 55°C) electrophoresis, respectively. Gels were stained with Ultra GelRed (Vazyme) or SUPER Green II (Starleaf) and visualized on ChemiDoc XRS+ System (Bio-Rad). RiboRuler High Range RNA Ladder (ThermoFisher) and DL2000 DNA Marker (Takara) were used as size markers.

Calculation of ligation yield and overall yield

Ligation yield calculations were dependent on the relative molar quantities determined on PAGEs. After the bands of the product and by-products were determined based on their molecular sizes and mobility on PAGE, their intensities (I) of the perfectly ligated product (P, the desired one) and the imperfectly ligated products (by-products: P_1, …, P_n) from the selected substrate (S; all RNA substrates were in equal molar quantities and we choose the longest one) were quantified by the ImageLab software (Bio-Rad). The intensities of these gel bands were represented by 'I_S' for S, 'I_P' for P and 'I_{P1}' to 'I_{Pn}' for P_1 to P_n. As they are correlated linearly with the RNA weights, the band intensities could serve as the relative weights of the corresponding RNAs, whose ratios to their molar masses (M) could be regarded as the relative molar quantities. The ligation yields were calculated as the ratio of the actual ligation product quantity (equal to the relative molar quantity of the perfectly ligated product) to the theoretical quantity (equal to the sum of the relative molar quantities of the substrate and its derivatized products) and the equation was shown as follows:

$$\text{ligation yield}\ (\%) = \frac{\frac{I_P}{M_P}}{\frac{I_S}{M_S} + \frac{I_P}{M_P} + \frac{I_{P1}}{M_{P1}} + \cdots + \frac{I_{Pn}}{M_{Pn}}} \times\ 100.$$

Overall yields were calculated as the ratio of the actual output molar quantity (n_{actual}) of the HPLC-purified mRNA product to the theoretical maximum output molar quantity ($n_{\text{theoretical}}$), which was calculated with the input of the longest substrate. n_{actual} was determined based on absorbance measured at 260 nm using a UV spectrophotometer (Multiskan, Thermo Fisher).

$$\text{overall yield}\ (\%) = \frac{n_{\text{actual}}}{n_{\text{theoretical}}} \times\ 100.$$

Purification of ligated RNAs

Ligated RNA products were purified through size-exclusion high-performance liquid chromatography (SEC-HPLC). Specifically, LiCl-precipitated RNA was redissolved, denatured at 75°C for 5 min and subjected to HPLC purification using SEC columns from Sepax Technologies (column 1: 4.6 mm × 300 mm, particle size of 5 μm, pore size of 2000 Å; or column 2: 4.6 mm × 300 mm, particle size of 5 μm, pore size of 1000 Å) on a 1260 Series HPLC (Agilent). The purification was performed with RNase-free TE buffer (10 mM Tris, 1 mM EDTA, pH 6) at a flow rate of 0.2 ml/min under denaturing conditions, and detected by UV absorption at 260 nm. Collected fractions were desalted and concentrated via ultrafiltration with 3-kDa ultrafiltration spin columns (Millipore) and analyzed via urea-PAGE.

RNA structure prediction

RNA structure prediction employed mFold (33) with default parameters.

Transfection and luminescence assay

SiHa cells (10 000 cells/well) were seeded in 96-well plates. Once cell confluency reached over 90%, cells were transfected with either 1.5 ng Gaussia luciferase mRNA or 15 ng LuxSit-i luciferase mRNA (34) using Lipofectamine 3000 (Invitrogen) as previously described (35). Specifically, 1 μl of mRNA and 0.2 μl of Lipofectamine 3000 were diluted in separate Opti-MEM medium (5 μl), followed by gentle tapping and incubation for 10 min at room temperature. The two dilutions were then combined, incubated for another 15 min at room temperature and added to the cells. Protein expression was assessed via luciferase assay with 2 μM coelenterazine for Gluc and 20 μM diphenylterazine for LuxSit-i, and luminescence was detected on a plate reader (Varioskan LUX, Thermo Fisher) (34).

Quantitative real-time reverse-transcription PCR

Total RNAs were extracted from cells using the Cell Total RNA Isolation Kit (Foregene). Quantitative real-time reverse-transcription PCRs (RT-qPCRs) were performed using the HiScript II One Step qRT-PCR SYBR Green Kit (Vazyme) with 0.2 ng/μl RNA sample on LC96 (Roche). Sequences of primer for quantification of cytokines are displayed in Supplementary Table S3. The thermocycling conditions were the following: reverse transcription incubation at 55°C for 5 min, initial denaturing at 95°C for 60 s, amplification for 40 cycles, including denaturing at 95°C for 10 s, extension at 60°C for 30 s. Following amplification, melting analysis was performed: 95°C for 60 s, 65°C for 60 s, melting from 65 to 97°C with a 0.2°C/s ramp, and 25 readings/s acquisition.

Statistical analysis

Unless otherwise specified, data are presented as mean ± standard error (SE). Statistical analysis and graphing were conducted using Prism 9 (GraphPad).

Results

The working principle of the DALI strategy

As shown in Figure 1, a plasmid containing the gene of interest is constructed and used to generate both the long dsDNA

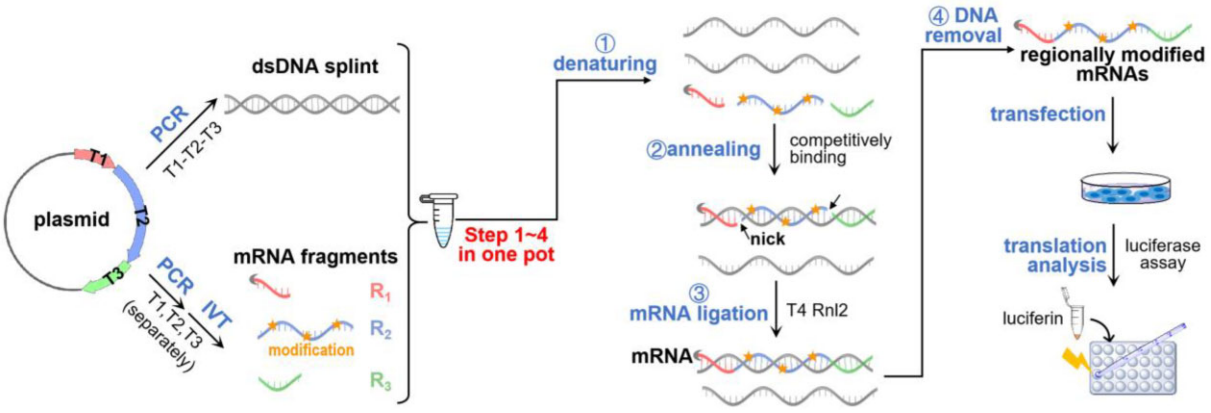

Figure 1. Scheme of the DALI strategy and its application on mRNA translation. A three-RNA ligation is shown as an example.

splint and the DNA templates for transcribing mRNA fragments. Subsequently, the transcribed mRNA fragments and the dsDNA splint are added in one pot, followed by denaturing and annealing treatments, to form a nicked RNA/DNA hybrid. This nick is ligated by T4 Rnl2, and the dsDNA splint is removed by digestion. Based on this strategy, the regionally modified mRNA can be efficiently synthesized and further transfected into cells to investigate its translation.

dsDNA splint can be used for RNA ligation and cyclization

To confirm the formation of splint DNA/mRNA fragment duplex, which was crucial for accurate ligation, an ssRNA (699 nt, R3) and a corresponding dsDNA (1146 bp) underwent a denaturing–annealing process, followed by a DNase I or RNase H digestion. The results unequivocally revealed that the RNA/DNA hybrid was formed, and the denaturing–annealing treatment was necessary for the hybrid formation (Figure 2A). In order to further verify whether the thermodynamic stability difference drove the competitive formation of the RNA/DNA hybrid from an ssRNA/dsDNA mixture, a high-resolution melting analysis of the annealed R3/DNA was conducted (Supplementary Figure S1). The experimental melting result (increased T_m by 0.7°C) of annealing DNA/RNA (versus dsDNA) indicated the formation of the RNA/DNA hybrid with higher thermal stability as reported (30,31). Further, by investigating the hybrid formation of mRNAs with different 3′ ends (sequences shown in Supplementary Tables S1 and S2), we found that the RNAs with unstructured terminal regions (such as polyA or non-stem sequence with low GC content) could allow easy hybrid formation between the mRNA fragments and the corresponding dsDNA (Supplementary Figure S2).

Motivated by the promising results above, we explored the capabilities of the dsDNA splints in assisting the ligation of long mRNA fragments. Initially, we investigated long dsDNA splinted multi-mRNA-fragment ligation, including two-, three- and four-RNA ligations (Figure 2B–D). We found that the 20-nt ssDNA splints whose lengths are widely used in ligation splints (21,22,24,36) barely offered any products, while the longer 59-nt ssDNA splints offered more products, indicating that the longer splints were more effective in guiding long RNA ligations (Figure 2B–D). As expected, much longer dsDNA (>1000 bp) effectively guided RNA ligations, resulting in a higher yield compared to all of the ssDNA splints (Figure 2B–D). In addition, we investigated the self-ligation (circularization) of one mRNA using a long dsDNA splint, where the substrate RNA and the dsDNA splint were obtained from different plasmids, unlike the multi-fragment ligation shown in Figure 1. The results demonstrated the success of the circularization, and the higher efficiency of long dsDNA splint in RNA circularization, compared to the ssDNA splint (Supplementary Figure S3). These observations demonstrated the advantage of using long dsDNA splints in ligating multiple large mRNA fragments and circularization.

dsDNA-splinted ligations exhibit high tolerance for structured substrates

To further investigate the efficiency of long dsDNA in ligating structured mRNA fragments, we conducted two-RNA ligation reactions using R5 and R6 fragments, which contained stable structures around the ligation ends (Supplementary Figure S4). The results indicated that, as expected (Figure 2E), the presence of stably folded structures at the ligation sites impeded RNA ligation guided by ssDNA splints. In contrast, the ligation using a long dsDNA splint exhibited a much better ligation efficiency. In particular, it exhibited over 33-, 20- and 6-fold improvement compared to the 20-, 59- and 89-nt ssDNA splints, respectively, revealing the potential of the long dsDNA strategy in ligating structured mRNA fragments.

Condition optimizations to establish the DALI strategy

To develop the DALI strategy for the general and efficient ligation of multiple mRNA fragments, we systematically optimized several conditions (Figure 3 and Supplementary Figure S5), including hybridization buffer, denaturing temperature, dsDNA format (linear or supercoiled), reaction duration, RNA ligase usage, RNA 3′-nucleotide, substrate length and additives. The results highlighted that one commercial buffer (Com; Beyotime) and two buffers (developed by our laboratory: Buffer-1 and Buffer-2, with compositions listed in the Figure 3 legend) enabled efficient ligations (Figure 3A). Additionally, the denaturing–annealing process greatly influenced ligation yield (Figure 3B). Specifically, at lower denaturation temperatures (60–85°C), the desired product (R2-3-4) was not formed. Instead, a longer product (R3 + R3) and an intermediate product (R3 + R4) were formed. The desired ligation products (R2-3-4) were generated at both 90°C

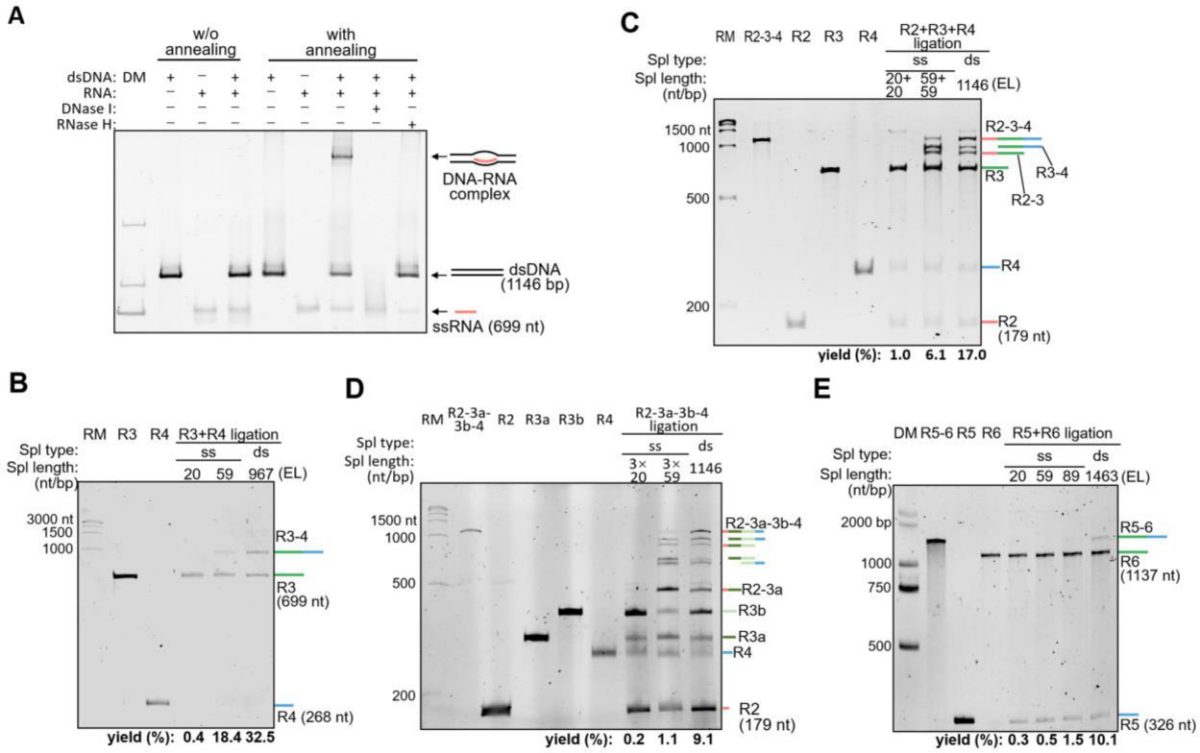

Figure 2. dsDNAs can be used as splints for mRNA ligations and can offer much more efficiency. (**A**) Native PAGE analysis of the formation of DNA/RNA hybrid. (**B**) Two-RNA ligations. (**C**) Three-RNA ligations. (**D**) Four-RNA ligations. ssDNA-splinted ligations used two or three ssDNA splints with the same lengths in each three- or four-RNA ligation, respectively, while the dsDNA-splinted ligations used only one. R3a and R3b are two fragments of R3 and are marked in different green colors. The yield was calculated based on the substrate R3a and its derived products. (**E**) Structured RNA ligations. Urea-denaturing PAGE was used to analyze the reactions in panels (B)–(E). 'Spl', 'DM', 'RM' and 'EL' refer to the ligation splints, DNA maker (DL2000, Takara), RNA maker (RiboRular High Range RNA ladder, Thermo Fisher) and equal in length to the desired ligated product, respectively. The splint and each RNA substrate in panels (B)–(E) were in equal molar ratios.

(optimal) and 95°C. However, intermediate products (R2 + R3 and R3 + R4) were also produced. These results with annealing buffers and temperatures highlighted the importance of the hybridization process on RNA ligation. Further, to assess the suitability of plasmids as splints, we performed the R5 + R6 ligation guided by the corresponding supercoiled plasmid and its linearized dsDNA. The results revealed that both linearized and supercoiled plasmid DNAs (4292 bp, longer than the length of the desired RNA product, 1463 nt) could function as splints, although they offered slightly lower yields than the dsDNA splint with the equal length (1463 bp) (Figure 3C). Furthermore, the reaction time and T4 Rnl2 usage were optimized to 2 h and 0.4 U/μl, respectively (Supplementary Figure S5A and B). Moreover, to optimize the ligation design, we investigated the efficiency preferences of RNA fragments with different lengths and ligation sites. The results revealed that the ligations with RNAs containing different lengths (Supplementary Figure S5C) and different 3′-nucleotides (Supplementary Figure S5D) exhibited comparable efficiencies, indicating that the ligation has no sequence preference.

To further enhance the efficiency of the dsDNA-splinted mRNA ligation, we tested various ligation additives. Large-molecule crowding agents (PEG8000 and PEG400), small-molecule crowding agents (trehalose and betaine) and chaotropes (TMAC, urea, DMSO and DMF) were added during the annealing process to promote hybrid formation, while the enzyme RppH (37) was supplemented in the ligation process to convert triphosphorylated mRNAs generated in GMP co-transcription (38) to active monophosphorylated form. Ligation yield analysis indicated that most additives significantly increased ligation efficiency; for instance, DMSO produced a relatively high yield of desired products and minimal nonspecific products (R6-6; Figure 3D). Following concentration optimization (Figure 3E), 20% DMSO combined with RppH was chosen for optimal ligation efficiency.

Based on these optimized conditions, we established the DALI strategy as follows: initially, an equal molar of RNA fragments and a corresponding dsDNA splint (its size equal to total length of all combined RNA fragments) are mixed in the annealing buffer (the commercial buffer or Buffer-1) with 20% DMSO; subsequently, the mixture is denatured and annealed by heating to 90°C for 1 s and then cooling to 25°C gradually at a rate of 0.02°C/s; finally, the ligation reaction is initiated by supplementing 0.4 U/μl T4 Rnl2 and incubated at 25°C for 2 h with RppH.

The ligation efficiency of the DALI strategy is superior to the ssDNA methods

To evaluate DALI capability, structured and multi-RNA ligations were performed. The results of structured-RNA ligations revealed that with identical lengths (20, 59 and 89 nt/bp), dsDNA splint-guided ligations exhibited generally higher efficiencies compared to the corresponding ssDNA-guided reactions (Figure 4A and B). In addition, as the length of the dsDNA splints increased from 20 to 1463 bp, the ligation yields escalated from 0.6% to 31.8%. Excitingly, DALI dramatically increased the ligation efficiency up to 31.8% yield, which was 106-, 64- and 19-fold over the traditional

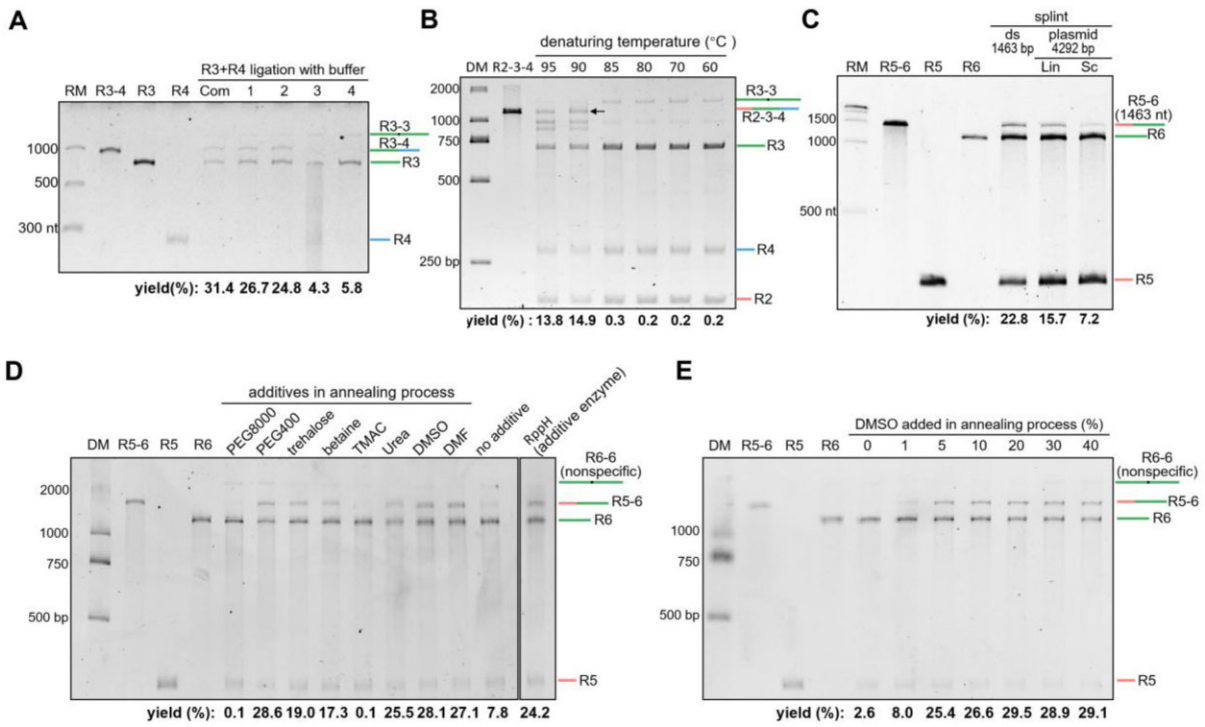

Figure 3. Optimizations of dsDNA-splinted mRNA ligation. (**A**) Optimization of hybridization buffer. Com: a commercial buffer (annealing buffer for RNA oligos) acquired from Beyotime; Buffer-1: 10 mM Tris–HCl (pH 8.0), 20 mM NaCl; Buffer-2: Buffer-1 with supplementary 1 mM EDTA; Buffer-3: 100 mM KOAc, 30 mM HEPES–KOH, 2 mM $Mg(OAc)_2$; Buffer-4: 50 mM sodium citrate. (**B**) Optimization of denaturing temperature. (**C**) Optimization of dsDNA splint format. (**D**) Optimization of additives. Additives in the annealing process: 5% PEG8000, 20% PEG400, 0.2 M trehalose, 1 M betaine, 40 mM tetramethylammonium chloride (TMAC), 1 M urea, 10% dimethylsulfoxide (DMSO) and 10% N,N-dimethylformamide (DMF); the additive in ligation: RppH (1 U for 1 μg RNA). (**E**) Optimization of DMSO usage.

20-, 59- and 89-nt ssDNA splints, respectively (Figure 4A and B, and Supplementary Figure S6A). Further, in ligating multiple mRNA fragments, DALI increased yields up to 27.2%, which was 6.0-, 2.8- and 1.9-fold over the traditional 20-, 59- and 89-nt ssDNA splints, respectively (Figure 4C and D, and Supplementary Figure S6B). Therefore, the DALI strategy marked a notable advancement, revealing high efficiency and generality in ligating multiple long mRNA fragments.

Regional modifications of mRNA exhibit different translation efficiencies and immunogenicity

Leveraging the advantages of DALI, the $m^1\psi$ regionally modified mRNAs encoding Gussia luciferase (GLuc) were successfully and efficiently synthesized for investigating the effect of mRNA regional modification on translation. To ensure the translatability of the produced mRNA in eukaryotes, capped mRNAs are generated through co-transcriptional with cap analog (CleanCap). The ligated mRNAs underwent HPLC analysis (Supplementary Figure S7A), HPLC purification (Supplementary Figure S7B), quantity analysis (Supplementary Figure S7C and D) and sequence analysis (Supplementary Figure S7E) before being transfected into cultured SiHa cells (Figure 5A). mRNA translation efficiencies were assessed through GLuc assays at 24 h post-transfection. We found that only the 3′UTR-modified mRNAs exhibited higher translation yields than the unmodified mRNA (Figure 5B). Further, compared with the fully modified mRNA, the relative translation efficiencies of mRNAs modified in 5′UTR, CDS and 3′UTR were 1.34-, 0.34- and 1.66-fold, respectively (Supplementary Figure S8A). These results indicated that the 3′UTR modification was advantageous, while the CDS modification was disadvantageous to translation efficiency. Furthermore, after 48 h post-transfection, the 3′UTR-modified and fully modified mRNAs had higher translation efficiency than the unmodified mRNA (Figure 5B and D), demonstrating their sustained translation. The 5′UTR-modified mRNAs (0.75-fold) and CDS-modified mRNAs (0.36-fold) exhibited lower translation efficiency than the fully modified one (Supplementary Figure S8A). Even worse, the CDS-modified and fully modified mRNAs could cause the formation of codon-shifted by-product proteins (15), indicating the need to avoid $m^1\psi$ modifications in CDS.

Moreover, we found that compared with the fully modified mRNAs, the 3′UTR $m^1\psi$-modified mRNA had higher translation efficiency (Figure 5B and D), while the 5′UTR and CDS non-modifications caused higher immunogenicity (Figure 5C and E). The potential immunogenicity of the unmodified regions was studied by RT-qPCR analysis of three immune factors (IL-6, IL-8 and TNF-α), and we have found that the 3′UTR-$m^1\psi$-modified mRNA had lower immunogenicity than unmodified mRNA (Unm), but the unmodified regions triggered immune responses (Figure 5C). To mitigate these, we decided to ligate three mRNA fragments with different modifications ($m^1\psi$ and m^5C). Thus, we synthesized mRNAs with the mixed modifications, including Mix1 mRNA (with 5′–3′UTR $m^1\psi$ modifications and CDS m^5C modifications) and Mix2 mRNA (with 5′UTR-CDS m^5C modifications and 3′UTR $m^1\psi$ modifications). These mRNAs encode LuxSit-i luciferase (34), whose translations were measured via luciferase activity assays. We have discovered that compared with the

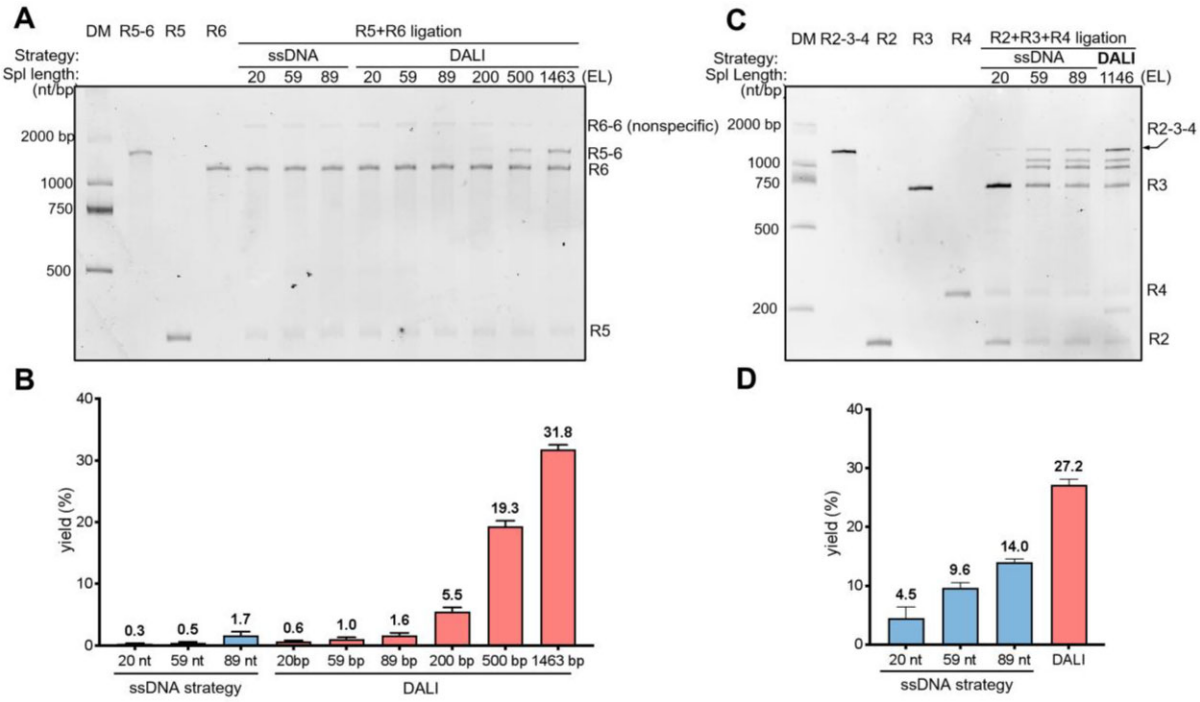

Figure 4. DALI efficiency in mRNA ligation compared to the ssDNA strategy. Urea-PAGE (**A**) and quantitative (**B**) analysis of structured-RNA ligations. The quantitative data were from PAGE analysis in Figure 4A and Supplementary Figure S6A. Urea-PAGE (**C**) and quantitative (**D**) analysis of multi-RNA ligations. Each three-RNA ligation using the ssDNA strategy contained two splints with the same lengths, while the DALI strategy used only one splint in a ligation. The quantitative data were from PAGE analysis in Figure 4C and Supplementary Figure S6B. Means and standard errors from three independent experiments are shown in each panel in Figure 4B and D.

full-length-m$^1\psi$ modified mRNAs (the canonical one), Mix1 and Mix2 had higher translation yields, especially Mix2 with a 2.35-fold increase after the 48-h post-transfection (Figure 5D and Supplementary Figure S8B). Additionally, the mRNA immunogenicity was significantly reduced by the combined m$^1\psi$ and m^{5}C modifications, particularly in the case of Mix2 mRNA (Figure 5E). Thus, the regional-specifically modified mRNAs (for instance, with the 3′UTR-m$^1\psi$ and 5′UTR/CDS-m^{5}C modifications) are advantageous to mRNA therapeutics with high translation efficiency and low immunogenicity.

Discussion

Global chemical modifications (such as m$^1\psi$ and m^{5}C) on mRNAs have shown their benefits on mRNA therapeutics by reducing immunogenicity, increasing stability and augmenting translation activity (39,40). Unfortunately, recent investigations revealed that the global modifications can cause side effects, such as translation rate decrease and codon frameshifting caused by CDS modifications (15,41). Since the exact impacts of the region modifications are unclear, it is essential to modify mRNA region-specifically, in order to improve the mRNA performance in translation efficiency, accuracy and immunogenicity. However, the region-specific mRNA synthesis is challenging. To address this, we have developed the DALI strategy, a robust method utilizing easily prepared dsDNA to *in situ* form nick hybrid and facilitate mRNA ligation in one pot.

Double-stranded nick structure formation

Since T4 Rnl2 ligase activity depends on the assembled nick structure (24), the formation of this structure becomes the limiting step for efficient ligation of long RNAs. Heating and cooling the mixture of the long RNA fragments and the dsDNA caused denaturing of folded RNA and dsDNA, and annealing of multi-RNA/DNA duplex (the nick structure), since the RNA/DNA hybrid is more thermostable over the folded RNA and the dsDNA (Supplementary Figure S1), consistent with other reports (30,31). Our results confirmed that the one-pot denaturing–annealing process is well suited for directly forming this nick structure in the reaction mixture of dsDNA and long RNA fragments (Figure 2A).

Effect of splint lengths on mRNA fragment ligation

Based on our above analysis and experimental results, longer splints of either ssDNAs or dsDNAs were more effective in guiding long RNA ligation (Figures 2 and 4). Substrate mRNA fragments tend to fold into complex structures that hinder short DNA splint binding and prevent the nick structure formation. Further, longer splints can pair the RNA within a broader range of sequences, especially starting from the unstructured ‘seed’ regions of the long RNA (Supplementary Figure S2). This initial pairing between the long splint and the ‘seed’ can form first and be extended, which allows ssDNA to compete with the folded RNA, indicating that longer splints are better than shorter ones.

Effects of regional modifications on mRNA translation and immunogenicity

The effects of modifications on mRNA translation are multifaceted, influencing the translation yield (42), rate (15,41), turnover (21), accuracy (15), mRNA immunogenicity (40,41) and mRNA secondary structure stability (42). For instance, m$^1\psi$ modifications can decrease accuracy (15) and

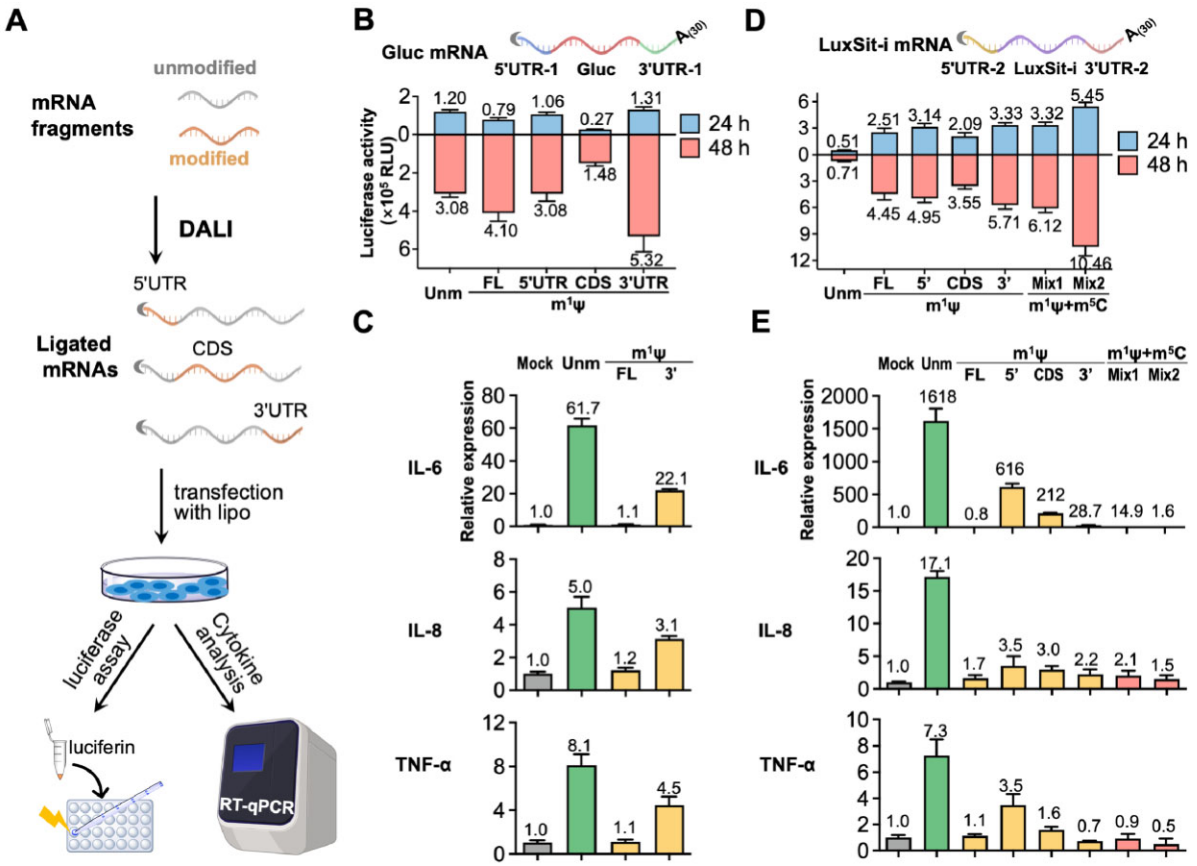

Figure 5. DALI-enabled investigations of regionally modified mRNAs on translation efficiency and immunogenicity. (**A**) Schematic overview of DALI-enabled workflow. Luciferase assay measuring expression levels of region-specifically modified mRNAs encoding Gluc luciferase (**B**) and LuxSit-i luciferase (**D**). $n = 4$. 'Mix1' was the mRNA with the 5′/3′UTR $m^1\psi$ modifications and CDS m^5C-modifications and 'Mix2' was the mRNA with the 5′UTR-CDS m^5C-modifications and 3′UTR $m^1\psi$ modifications. RT-qPCR analysis of IL-6, IL-8 and TNF-α expression after 24 h of transfection with GLuc mRNAs (**C**) or LuxSit-i mRNAs (**E**). $n = 3$.

slow down translation elongation (15,41), while increasing mRNA translation yield (40–42) and reducing immunogenicity (8). To investigate these effects in specific mRNA regions, we assessed the translation efficiency, immunogenicity and serum stability of mRNAs with the region-specific $m^1\psi$ and m^5C modifications. Our results indicated that these modifications had minimal impact on mRNA stability in serum (Supplementary Figure S9), suggesting that their nuclease resistance did not directly correlate with the translation efficiency and yield of these modified mRNAs. In terms of regional modification effect on translation, we have found that $m^1\psi$ modification in the CDS region significantly inhibited translation (Figure 5B and D), while this modification in the 3′UTR region enhanced translation. It has been reported that the CDS-region modifications reduce translation rate (15,41) and increase decoding errors (15), whereas 3′UTR modifications stabilize secondary structures that support efficient translation (42). Our results and the literature report on $m^1\psi$ modification-induced inaccuracy (15) have suggested that instead of CDS, 3′UTR is a suitable region for $m^1\psi$ modification. Further, our immunogenicity investigations have suggested that limiting $m^1\psi$ modifications to specific regions may significantly reduce the immune responses, and placing $m^1\psi$ modifications in a smaller 3′UTR region may offer more immunogenicity reduction than in a larger CDS region (Figure 5E). This suggests that the reduction may be influenced by both the modification region sizes and sequences. Interestingly, the region-specific mRNAs with the mixed modifications ($m^1\psi$ in the 3′UTR and m^5C in the 5′UTR and CDS) showed relatively high translation yield and relatively low immunogenicity, underscoring the region-specific effects of these modifications. Our experimental results have highlighted the need for thorough investigations into the regional modifications and their impacts on mRNA translation efficiency and immunogenicity, providing insights into the translation fundamental mechanisms and mRNA therapeutic discoveries.

Conclusion

To synthesize regionally modified mRNAs, we have devised an efficient and convenient strategy (DALI) that uses a long dsDNA as a ligation splint to overcome the challenge of low efficiency in ligating multiple mRNA fragments. The long dsDNA splints can be easily prepared in various lengths for suppressing the formation of self-folded RNA structures. Consequently, our strategy can dramatically increase the efficiency for ligating mRNA fragments, especially for structured ones, by up to 106-fold over the ssDNA strategy. Using DALI, we efficiently synthesized mRNAs with region-specific $m^1\psi$ modifications or $m^1\psi/m^5C$ mixed modifications to investigate translation and immunogenicity. Compared with mRNAs modified with $m^1\psi$ in full length (the canonical modification style), the 3′UTR-$m^1\psi$-modified mRNAs had higher translation efficiency, whereas the CDS- or 5′UTR-$m^1\psi$-modified mRNA

exhibited lower efficiency. Moreover, we have demonstrated that the regionally modified mRNAs containing the combined 3′UTR-$m^1\psi$ and 5′UTR/CDS-m^5C modifications offered high translation efficiency and low immunogenicity. In general, our DALI methodology holds promise for advancing mRNA research and therapeutic applications.

Data availability

The data underlying this article are available in the article and in its online supplementary material.

Supplementary data

Supplementary Data are available at NAR Online.

Funding

National Key R&D Program of China [2023YFC3403200, 2022YFC2303700]; National Natural Science Foundation of China [22107079, 22077089]; Sichuan Province Science and Technology Support Program [2022YFSY0013, 2023NSFSC1107]; China Postdoctoral Science Foundation [2020M673205]; Open Research Fund of State Key Laboratory of Southwest Chinese Canonical Medicine Resources [SKLTCM202301]. Funding for open access charge: National Key R&D Program of China [2023YFC3403200].

Conflict of interest statement

None declared.

References

1. Qin,S., Tang,X., Chen,Y., Chen,K., Fan,N., Xiao,W., Zheng,Q., Li,G., Teng,Y., Wu,M., *et al.* (2022) mRNA-based therapeutics: powerful and versatile tools to combat diseases. *Signal Transduct. Target. Ther.*, **7**, 166.
2. Watson,O.J., Barnsley,G., Toor,J., Hogan,A.B., Winskill,P. and Ghani,A.C. (2022) Global impact of the first year of COVID-19 vaccination: a mathematical modelling study. *Lancet Infect. Dis.*, **22**, 1293–1302.
3. Wang,X., Liu,C., Rcheulishvili,N., Papukashvili,D., Xie,F., Zhao,J., Hu,X., Yu,K., Yang,N., Pan,X., *et al.* (2023) Strong immune responses and protection of PcrV and OprF-I mRNA vaccine candidates against *Pseudomonas aeruginosa*. *npj Vaccines*, **8**, 76.
4. Rojas,L.A., Sethna,Z., Soares,K.C., Olcese,C., Pang,N., Patterson,E., Lihm,J., Ceglia,N., Guasp,P., Chu,A., *et al.* (2023) Personalized RNA neoantigen vaccines stimulate T cells in pancreatic cancer. *Nature*, **618**, 144–150.
5. Weber,J.S., Carlino,M.S., Khattak,A., Meniawy,T., Ansstas,G., Taylor,M.H., Kim,K.B., McKean,M., Long,G.V., Sullivan,R.J., *et al.* (2024) Individualised neoantigen therapy mRNA-4157 (V940) plus pembrolizumab versus pembrolizumab monotherapy in resected melanoma (KEYNOTE-942): a randomised, phase 2b study. *Lancet*, **403**, 632–644.
6. Koeberl,D., Schulze,A., Sondheimer,N., Lipshutz,G.S., Geberhiwot,T., Li,L., Saini,R., Luo,J., Sikirica,V., Jin,L., *et al.* (2024) Interim analyses of a first-in-human phase 1/2 mRNA trial for propionic acidaemia. *Nature*, **628**, 872–877.
7. Robinson,E., MacDonald,K.D., Slaughter,K., McKinney,M., Patel,S., Sun,C. and Sahay,G. (2018) Lipid nanoparticle-delivered chemically modified mRNA restores chloride secretion in cystic fibrosis. *Mol. Ther.*, **26**, 2034–2046.
8. Karikó,K., Buckstein,M., Ni,H. and Weissman,D. (2005) Suppression of RNA recognition by toll-like receptors: the impact of nucleoside modification and the evolutionary origin of RNA. *Immunity*, **23**, 165–175.
9. Nelson,J., Sorensen,E.W., Mintri,S., Rabideau,A.E., Zheng,W., Besin,G., Khatwani,N., Su,S.V., Miracco,E.J., Issa,W.J., *et al.* (2020) Impact of mRNA chemistry and manufacturing process on innate immune activation. *Sci. Adv.*, **6**, eaaz6893.
10. Moradian,H., Roch,T., Anthofer,L., Lendlein,A. and Gossen,M. (2022) Chemical modification of uridine modulates mRNA-mediated proinflammatory and antiviral response in primary human macrophages. *Mol. Ther. Nucleic Acids*, **27**, 854–869.
11. Edupuganti,R.R., Geiger,S., Lindeboom,R.G.H., Shi,H., Hsu,P.J., Lu,Z., Wang,S.-Y., Baltissen,M.P.A., Jansen,P.W.T.C., Rossa,M., *et al.* (2017) N^6-Methyladenosine (m^6A) recruits and repels proteins to regulate mRNA homeostasis. *Nat. Struct. Mol. Biol.*, **24**, 870–878.
12. Creech,C.B., Anderson,E., Berthaud,V., Yildirim,I., Atz,A.M., Melendez Baez,I., Finkelstein,D., Pickrell,P., Kirstein,J., Yut,C., *et al.* (2022) Evaluation of mRNA-1273 Covid-19 vaccine in children 6 to 11 years of age. *N. Engl. J. Med.*, **386**, 2011–2023.
13. Thomas,S.J., Moreira,E.D. Jr, Kitchin,N., Absalon,J., Gurtman,A., Lockhart,S., Perez,J.L., Pérez Marc,G., Polack,F.P., Zerbini,C., *et al.* (2021) Safety and efficacy of the BNT162b2 mRNA Covid-19 vaccine through 6 months. *N. Engl. J. Med.*, **385**, 1761–1773.
14. Croce,S., Serdjukow,S., Carell,T. and Frischmuth,T. (2020) Chemoenzymatic preparation of functional click-labeled messenger RNA. *ChemBioChem*, **21**, 1641–1646.
15. Mulroney,T.E., Poyry,T., Yam-Puc,J.C., Rust,M., Harvey,R.F., Kalmar,L., Horner,E., Booth,L., Ferreira,A.P., Stoneley,M., *et al.* (2024) N^1-Methylpseudouridylation of mRNA causes +1 ribosomal frameshifting. *Nature*, **625**, 189–194.
16. Petkovic,S. and Mueller,S. (2015) RNA circularization strategies *in vivo* and *in vitro*. *Nucleic Acids Res.*, **43**, 2454–2465.
17. Nakamoto,K., Abe,N., Tsuji,G., Kimura,Y., Tomoike,F., Shimizu,Y. and Abe,H. (2020) Chemically synthesized circular RNAs with phosphoramidate linkages enable rolling circle translation. *Chem. Commun.*, **56**, 6217–6220.
18. Kollaschinski,M., Sobotta,J., Schalk,A., Frischmuth,T., Graf,B. and Serdjukow,S. (2020) Efficient DNA click reaction replaces enzymatic ligation. *Bioconj. Chem.*, **31**, 507–512.
19. Bullard,D.R. and Bowater,R.P. (2006) Direct comparison of nick-joining activity of the nucleic acid ligases from bacteriophage T4. *Biochem. J.*, **398**, 135–144.
20. Mueller,S. and Appel,B. (2017) *In vitro* circularization of RNA. *RNA Biol.*, **14**, 1018–1027.
21. Kawaguchi,D., Kodama,A., Abe,N., Takebuchi,K., Hashiya,F., Tomoike,F., Nakamoto,K., Kimura,Y., Shimizu,Y. and Abe,H. (2020) Phosphorothioate modification of mRNA accelerates the rate of translation initiation to provide more efficient protein synthesis. *Angew. Chem. Int. Ed.*, **59**, 17403–17407.
22. Abe,N., Matsumoto,K., Nishihara,M., Nakano,Y., Shibata,A., Maruyama,H., Shuto,S., Matsuda,A., Yoshida,M., Ito,Y., *et al.* (2015) Rolling circle translation of circular RNA in living human cells. *Sci. Rep.*, **5**, 16435.
23. Qu,L., Yi,Z., Shen,Y., Lin,L., Chen,F., Xu,Y., Wu,Z., Tang,H., Zhang,X., Tian,F., *et al.* (2022) Circular RNA vaccines against SARS-CoV-2 and emerging variants. *Cell*, **185**, 1728–1744.
24. Chen,H., Cheng,K., Liu,X., An,R., Komiyama,M. and Liang,X. (2020) Preferential production of RNA rings by T4 RNA ligase 2 without any splint through rational design of precursor strand. *Nucleic Acids Res.*, **48**, e54.
25. Nandakumar,J., Ho,C.K., Lima,C.D. and Shuman,S. (2004) RNA substrate specificity and structure-guided mutational analysis of bacteriophage T4 RNA ligase 2. *J. Biol. Chem.*, **279**, 31337–31347.
26. Hertler,J., Slama,K., Schober,B., Özrendeci,Z., Marchand,V., Motorin,Y. and Helm,M. (2022) Synthesis of point-modified mRNA. *Nucleic Acids Res.*, **50**, e115.

27. Hughes,R.A. and Ellington,A.D. (2017) Synthetic DNA synthesis and assembly: putting the synthetic in synthetic biology. *Cold Spring Harbor Perspect. Biol.*, **9**, a023812.
28. Praetorius,F., Kick,B., Behler,K.L., Honemann,M.N., Weuster-Botz,D. and Dietz,H. (2017) Biotechnological mass production of DNA origami. *Nature*, **552**, 84–87.
29. Jia,Y., Chen,L., Liu,J., Li,W. and Gu,H. (2021) DNA-catalyzed efficient production of single-stranded DNA nanostructures. *Chem*, **7**, 959–981.
30. Wang,P., Ko,S.H., Tian,C., Hao,C. and Mao,C. (2013) RNA–DNA hybrid origami: folding of a long RNA single strand into complex nanostructures using short DNA helper strands. *Chem. Commun.*, **49**, 5462–5464.
31. Ko,S.H., Su,M., Zhang,C., Ribbe,A.E., Jiang,W. and Mao,C. (2010) Synergistic self-assembly of RNA and DNA molecules. *Nat. Chem.*, **2**, 1050–1055.
32. Davanloo,P., Rosenberg,A.H., Dunn,J.J. and Studier,F.W. (1984) Cloning and expression of the gene for bacteriophage T7 RNA polymerase. *Proc. Natl Acad. Sci. U.S.A.*, **81**, 2035–2039.
33. Zuker,M. (2003) Mfold web server for nucleic acid folding and hybridization prediction. *Nucleic Acids Res.*, **31**, 3406–3415.
34. Yeh,A.H., Norn,C., Kipnis,Y., Tischer,D., Pellock,S.J., Evans,D., Ma,P., Lee,G.R., Zhang,J.Z., Anishchenko,I., *et al.* (2023) *De novo* design of luciferases using deep learning. *Nature*, **614**, 774–780.
35. Liang,X., Potter,J., Kumar,S., Zou,Y., Quintanilla,R., Sridharan,M., Carte,J., Chen,W., Roark,N., Ranganathan,S., *et al.* (2015) Rapid and highly efficient mammalian cell engineering via Cas9 protein transfection. *J. Biotechnol.*, **208**, 44–53.
36. Abe,N., Hiroshima,M., Maruyama,H., Nakashima,Y., Nakano,Y., Matsuda,A., Sako,Y., Ito,Y. and Abe,H. (2013) Rolling circle amplification in a prokaryotic translation system using small circular RNA. *Angew. Chem. Int. Ed.*, **52**, 7004–7008.
37. Deana,A., Celesnik,H. and Belasco,J.G. (2008) The bacterial enzyme RppH triggers messenger RNA degradation by 5′ pyrophosphate removal. *Nature*, **451**, 355–358.
38. Martin,C.T. and Coleman,J.E. (1989) T7 RNA polymerase does not interact with the 5′-phosphate of the initiating nucleotide. *Biochemistry*, **28**, 2760–2762.
39. Nance,K.D. and Meier,J.L. (2021) Modifications in an emergency: the role of N^1-methylpseudouridine in COVID-19 vaccines. *ACS Cent. Sci.*, **7**, 748–756.
40. Andries,O., Mc Cafferty,S., De Smedt,S.C., Weiss,R., Sanders,N.N. and Kitada,T. (2015) N^1-Methylpseudouridine-incorporated mRNA outperforms pseudouridine-incorporated mRNA by providing enhanced protein expression and reduced immunogenicity in mammalian cell lines and mice. *J. Control. Release*, **217**, 337–344.
41. Svitkin,Y.V., Cheng,Y.M., Chakraborty,T., Presnyak,V., John,M. and Sonenberg,N. (2017) N^1-Methyl-pseudouridine in mRNA enhances translation through eIF2α-dependent and independent mechanisms by increasing ribosome density. *Nucleic Acids Res.*, **45**, 6023–6036.
42. Mauger,D.M., Cabral,B.J., Presnyak,V., Su,S.V., Reid,D.W., Goodman,B., Link,K., Khatwani,N., Reynders,J., Moore,M.J., *et al.* (2019) mRNA structure regulates protein expression through changes in functional half-life. *Proc. Natl Acad. Sci. U.S.A.*, **116**, 24075–24083.

Received: April 17, 2024. **Revised:** December 9, 2024. **Editorial Decision:** December 11, 2024. **Accepted:** December 18, 2024